Cell Wall Property Changes of White Rot Larch during Decay Process

Weiwei Shangguan,[a] Haiqing Ren,[a] Jianxiong Lv,[a] Benhua Fei,[b] Zhangjing Chen,[c] Rongjun Zhao,[a,*] and Youke Zhao [a,*]

Larch flakes infested with white rot fungus were examined following several infestation durations with respect to the mass loss, tensile strength, hardness, porosity, and change in cell wall components. Nano-indentation, X-ray diffraction (XRD), nitrogen adsorption, and Fourier transform infrared (FTIR) spectroscopy testing methods were employed to investigate the property changes during the decay process. The testing results showed that the mass loss was greater and the longitudinal tensile strength decreased following the first three-week infestation. Nano-indentation measurements revealed that the average MOE of infested larch flakes decreased from 24.0 to 17.1 GPa and the average hardness declined from 528.47 to 427.87 MPa following 12 weeks of infestation. After the first three weeks, the relative crystallinity, surface area, and micropore area of the infested samples increased. These parameters decreased after three weeks had elapsed. Changes in the absorption peaks observed in FTIR explained that the first three-week infestation had a strong effect on the mass loss and strength changes. This suggests that white rot fungus intensely attacked the lignin component of the biomass during the first three weeks of infestation.

*Contact information: a: State Key Laboratory of Tree Genetics and Breeding, Research Institute of Wood Industry of Chinese Academy of Forestry, 1 Dong Xiao Fu, Xiang Shan Road, Hai Dian, Beijing, China, 100091; b: International Center for Bamboo and Rattan, Beijing, China, 100102; c: Department of Wood Science and Forest Products, Virginia Polytechnic Institute and State University, Blacksburg, VA 24060, USA; *Corresponding authors: rongjun@caf.ac.cn, youke.zhao@caf.ac.cn*

INTRODUCTION

Decaying wood exhibits degradation phenomena caused by microorganisms. There are two kinds of wood-decaying fungi: white rot and brown rot. White rot fungus destroys lignin and cellulose, leaving the rotted wood white or slightly yellow. Brown rot fungus attacks the carbohydrates of the wood cell wall, leaving reddish or brown decayed wood (Cowling 1961). Disintegration of wood by decaying fungi causes a loss of mechanical strength and cell wall changes that affect the end uses of the wood. The mechanical strength of wood decreases greatly during the early period of decay but changes less dramatically during the later stages of decay (Curling *et al.* 2002; Wilcox 1978; Winandy and Morrell 1993). The mass loss and density gradually decrease during the later stages of decay (Solár *et al*. 2007). Curling *et al.* (2002) studied the changes in mechanical properties by analyzing the components of the cell wall. He concluded that the strength losses (of less than 40%) in the early decay period were associated with the reduction of arabinose and galactose in the cell wall. However, strength losses (of more than 40%) during the later decay period were due to decreases in mannan and xylan.

White rot fungus attacks both lignin and cellulose, although different attacking rates may exist (Pandey and Pitman 2003). Perez *et al*. (1993) studied the effects of *Coriolus versicolor* on mass loss and lignin content. Xylan and lignin were degraded simultaneously during the decay of wood. However, the protein content in *Aextoxicon punctatum* wood increased, according to infrared spectroscopy. Davis *et al*. (1994) and Pandey and Pitman (2003) also reported that *C. versicolor* attacks both lignin and carbohydrates at the same time, with a slightly higher rate for lignin. Scanning electron microscopy was used by Blanchette *et al*. (1985) to detect the micromorphological and ultrastructural changes that occurred in wood cells during white rot degradation. The results showed that the compound middle lamella was extensively degraded in delignified areas, causing fibril separation. Perez *et al*. (1993) used solid-state nuclear magnetic resonance (NMR) spectra to study decayed wood; no changes in the solid-state ^{13}C NMR spectra were observed after wood was degraded by *C. versicolor.* Although white rot fungi attack decreases the mechanical properties of wood, this fungus can be used in making pulp and paper. Buchert *et al*. (1998) found that using white rot-treated pulp, the paper tensile index was increased by 49%, the tear index by 34%, and the internal bonding strength by 32%. Shao and Li (2006) reported that the lignin present on the fiber surface reduced the internal bond strength of the pulp fibers. Research related to the white rot attack of wood is valuable because its results can improve the uses of biomaterials and other natural resources.

The crystallinity of wood is defined as the weight fraction of the crystalline portion of the wood. The first quantitative investigation into the crystallinity of cellulose fibers using X-ray diffraction (XRD) was conducted by Hermans and Weidinger (1948). More recently, XRD has been used to calculate the crystallinity of wood (Andersson *et al*. 2003; Cutter *et al*. 1980). Li *et al*. (2011) successfully used XRD to analyze the crystallinity of brown rot-decayed wood. They found that the crystallinity of decayed wood decreased slowly during the initial stage and rapidly during the later stage of decay. Analysis of the pore volume (which is related to the cell wall) is crucial for understanding the mechanical properties of wood. This methodology has been used to evaluate cement-based materials (Kaufmann 2010), chemical materials (Westermarck *et al*. 1998), and wood (Chang *et al*. 2011). Kojiro *et al*. (2010) studied mesopores in the cell wall of dry wood using nitrogen gas adsorption and discovered that the mesopore volume barely changed with the elevation of pretreatment temperatures. Fourier transform infrared (FTIR) spectroscopy can be used to quantify the chemical composition of a material. It has been widely used in study of pulp, paper, and wood (Berben *et al*. 1987; Rodrigues *et al*. 1998; Schultz *et al*. 1985; Schwanninger *et al*. 2004). Research regarding changes of functional groups during wood decay has been carried out with FTIR (Fackler *et al*. 2006; 2010; Jones *et al*. 2011). Fackler *et al*. (2011) used FTIR to find that the cleavage of glycosidic bonds of polysaccharides preceded metabolization of white rot. A relative decrease of the overall lignin content and a relative accumulation of wood polysaccharides were also detected. Pandey and Pitman (2003) used FTIR to qualitatively and quantitatively examine changes in the lignin and carbohydrate components of wood. Nano-indentation strength, which can reflect the mechanical properties of untreated wood cell wall, has been studied since the nineties. Such studies were pioneered by Wimmer *et al*. (1997). Yu *et al*. (2010) investigated the mechanical properties of Masson pine (*Pinus massoniana*) with regards to moisture content (MC) using nano-indentation technology.

The objectives of this study were to investigate the tensile and nano-indentation properties of decayed larch flakes. Cellulose crystallinity, porosity, and chemical content, each affecting the mechanical properties of wood, were analyzed following several fungi

infestation durations. The results of this study provide new data, not only regarding the cell wall properties during white rot decay, but also for the bio-pulping and papermaking industries.

EXPERIMENTAL

Materials

White rot wood flake sample preparation

Clear larch (*Larix olgensis* Henry) samples with dimensions of 90 mm × 10 mm × 1.5 mm (longitudinal × radial × tangential) and 11.4% moisture content were cut from wood located at the 25th annual ring, where the mechanical properties were relatively consistent (Fig. 1). A total of 180 samples were cut from air-dried larch logs. The flake samples were separated into five groups, each with 36 samples, for different infestation durations: 0 (non-infested), 3, 6, 9, or 12 weeks. In each group, 12 samples were used for tensile strength testing, 12 were used for nano-indentation testing, and 12 were ground into powder that was used for XRD, nitrogen adsorption, and FTIR testing.
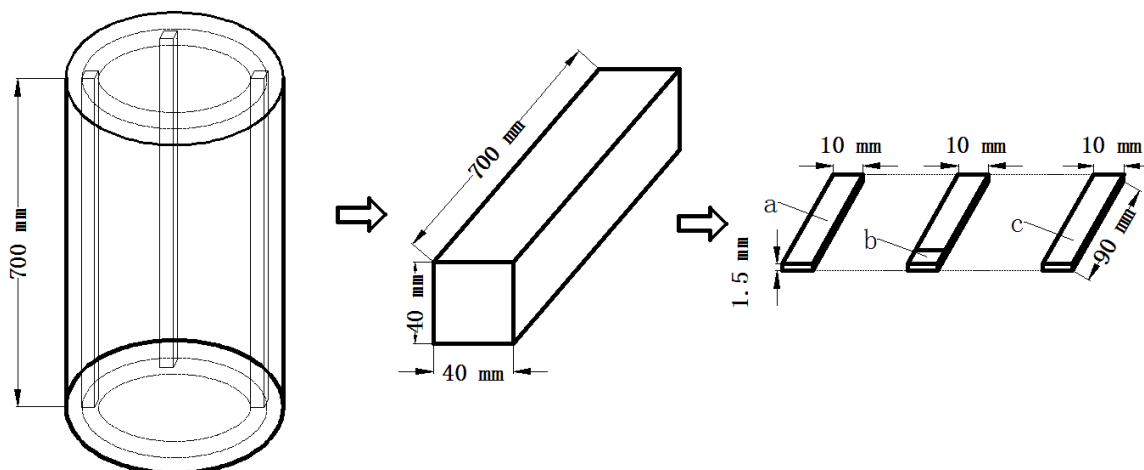
Fig. 1. Larch flake preparation: size and cutting pattern. (a) Tensile samples, (b) nano-indentation samples, (c) XRD, nitrogen adsorption, and FTIR samples

The white rot fungus *C. versicolor* was incubated and cultivated in malt agar substrate according to ASTM D 2017 (2005). The prepared larch flakes were inoculated with the cultivated fungus. The infested samples were kept in a chamber maintained at a constant temperature of 26 °C and humidity of 75% for infestation periods of 3, 6, 9, and 12 weeks.

Methods

Mass loss of white rot flakes

The samples were placed in an oven at 103 ± 3 °C for 8 h and weighed with an electronic balance with 0.1-mg precision before the flakes were inoculated with fungus. This weight was designated w_1. After each infestation period, *C. versicolor* on the sample surface was wiped off and the samples were placed in the oven at the same temperature for another 8 h until a constant weight (w_2) was achieved. The mass loss of the flakes was calculated as follows,

$$w = \frac{w_1 - w_2}{w_1} \times 100\% \qquad\qquad (1)$$

where w is the mass loss of the white rot flakes and w_1 and w_2 are the weights of the sample before and after infestation, respectively.

Tensile strength of white rot flakes

   C. versicolor on the sample surface was gently scraped off. Shims of dimensions 20 mm × 10 mm × 1.5 mm (length × width × thickness) were taken from *Cylicodiscus gabunensis* and attached to the ends of the samples with white latex (Fig. 2). The shims prevented breaking of samples in the area held by the clamp due to stress concentration. The samples were conditioned in a chamber at a constant temperature of 20 ± 2 °C and a relative humidity of 65 ± 5% for 24 h before they were evaluated. The machine used during this experiment was an Instron 5582 (Instron Co., Grove City, PA). The tensile speed was set to 2 mm/min during testing.

Fig. 2. Longitudinal tensile samples of larch flakes used for strength testing

Hardness of white rot flake measured with nano-indentation

   The nano-indentation technique can obtain the stress-strain curve of wood at the micro level, and be used to calculate the modulus of elasticity (MOE) and hardness of wood cell wall. The apparatus used in this experiment was a Nanoindenter XP made by the MTS Company (USA). This Berkovich indenter was equipped with a three-sided, pyramidal diamond tip and was loaded to 250 µN at a rate of 50 µN/s. The testing chamber was held at 22 °C and 45% relative humidity. Infested samples were processed to a pyramidal shape and were polished with a diamond knife (Fig. 3). Twenty indentations were tested for each infestation duration. The testing principles and methods are described in detail by Yu *et al*. (2010).

   The hardness can be calculated using Eq. (2) and the elastic modulus can be obtained using Eq. (3),

$$H = \frac{P}{A} \qquad\qquad (2)$$

$$\frac{1}{E_r} = \frac{1-v^2}{E} + \frac{1-v_i^2}{E_i} \tag{3}$$

where H is the hardness, P is the load of the indenter at the maximum indentation depth, and A is the projection area of the indentation at the maximum indentation depth. Also, E_i and v_i are the elastic modulus and the Poisson ratio of the tips, respectively; E_r is the reduced modulus measured by the instrument; E_i is 1141 GPa and v_i is 0.07 for diamond tips; E and v are the elastic modulus and Poisson ratio of samples, respectively. For this study, the longitudinal Poisson ratio of wood cell wall was assumed to be 0.40. In practice, it ranges from 0.37 to 0.47 (Gibson and Ashby 1997).

Fig. 3. Nano-indentation sample installation

Cellulose crystallinity of white rot flakes measured with XRD

Cellulose crystallinity is the mass fraction of crystalline cellulose within wood. It can be determined with XRD. The larch powders of three samples were mixed and placed on the tray in the X-ray diffractometer. Testing was repeated three times for each condition and the values were averaged. A $\theta/(2\theta)$ link-scanning method (in which the receiver rotated 2θ when the sample tray rotated θ) was used to generate the 2θ intensity curve. The scan range (2θ) was 4 to 40°. The relative crystallinity of cellulose in non-infested samples and white rot-infested samples was calculated according to the Segal method, as follows,

$$C_{rl} = \frac{(I_{002} - I_{am})}{I_{002}} \times 100\% \tag{4}$$

where C_{rl} is the crystallinity of the cellulose, I_{002} is the maximum intensity of the crystal diffraction angle, and I_{am} is the scattering intensity of the amorphous region.

Porosity of white rot flakes measured with nitrogen adsorption

Powders from flakes of each infestation duration were mixed. Nitrogen was used as the adsorption medium in the absorption apparatus. When the nitrogen molecules contacted with wood powder, they were adsorbed on the surface of the powder through surface free energy.

The BET formula, which is based upon the phenomenon of physical adsorption of gases on the external and internal surfaces of a porous material (Brunauer *et al.* 1938; Fagerlund 1973), was used to calculate the specific surface area of the samples, as shown below,

$$\frac{p}{V_d(p_0-p)} = \frac{1}{V_m C} + \frac{C-1}{V_m C}\frac{p}{p_0} \tag{5}$$

where p and p_0 are the balance pressure and saturated vapor pressure, respectively, V_d and V_m are the adsorption quantity and monolayer adsorption saturation capacity, respectively, and C is the adsorption heat of the first layer and is a constant related to the heat of condensation.

The fraction p/p_0 ranges from 0.05 to 0.35; V_d can be determined experimentally. By plotting $\frac{p}{V_d(p_0-p)}$ against $\frac{p}{p_0}$, a straight line was obtained. The slope of this line is a $= \frac{C-1}{V_m C}$, and the intercept is b $= \frac{1}{V_m C}$. Solving,

$$V_m = \frac{1}{a+b} \tag{6}$$

The surface area of a sample is,

$$S_g = V_m \times A \times \sigma_m \tag{7}$$

where S_g is the surface area, A is Avogadro's constant (6.023×10^{23}), and σ_m is the sectional area of N_2 (0.162 nm^2).

The T-plot method was used to calculate the micropore area of samples,

$$STSA = M \times 15.47 \tag{8}$$

where STSA is the micropore area obtained with the T-plot, M is the slope of V *vs.* t, and V and t are the nitrogen adsorption volume per gram and adsorption thickness, respectively. The conversion constant between gas and liquid nitrogen is 15.74.

Cell wall components measured with FTIR testing

A Nicolet Impact 410 apparatus (USA) was used for FTIR testing over an infrared spectral range of 4000 to 400 cm^{-1}. The larch powder from three infested flakes was scraped with a metal blade. Then, potassium bromide (KBr) disks were made from 2 mg of wood powder mixed in 200 mg of KBr. Tests were repeated five times for each flake sample.

A spectral range of 2000 to 800 cm^{-1} was observed in this experiment. The peak heights at 1637 cm^{-1} (representing lignin) and 1066 cm^{-1} (representing hemicellulose and cellulose) (Colom *et al.* 2003; Sarkanen *et al.* 1967) were compared to those of reference peaks to determine the relative changes in the structural components. Peaks at 1510, 1730, and 895 cm^{-1} correspond to lignin, hemicellulose, and cellulose, respectively. They were relatively consistent and were chosen as the reference peaks. The peak value was calculated using OMNIC software (Nicolet, USA).

RESULTS AND DISCUSSION
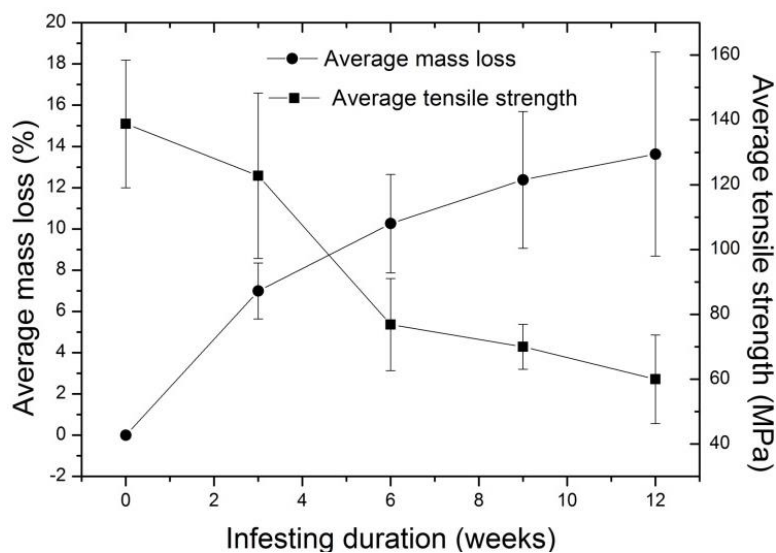
Mass Loss of White Rot Flakes

Table 1 shows the average mass loss of the larch flakes following each duration of infestation. The mass loss rate was greater in early decay, especially when the total mass loss was less than 10%. This is because the ligninolytic enzyme activity reaches a maximum at the beginning of decay and then decreases (Erwin *et al*. 1995). After week 6, the activity of the enzyme decreased, and the mass loss rate was thus reduced (Fig. 4).

Table 1. Average Mass Loss of Larch Flakes Infested with White Rot Fungus for Different Durations

Infestation Duration (Weeks)	Average Mass Loss (%)
3	7.00 (1.3)
6	10.25 (2.3)
9	12.38 (3.3)
12	13.63 (4.9)
Mean data (standard deviation)	

Tensile Strength of Infested Larch Flakes

Average mass loss and tensile strength as functions of the infestation time are shown in Fig. 4. The mass loss of larch flakes increased from 7.00 to 13.63% as the longitudinal tensile strength decreased from 138.8 to 60.0 MPa. The positive Pearson correlation between the mass loss and the tensile strength reduction was 0.949. The greater the mass loss, the more the tensile strength decreased. The cell wall of the wood is closely related to the mechanical strength of the wood. White rot fungus attacks the surfaces of micro-fibrils, destroying the crystalline and amorphous regions at the same time without substantially reducing the average chain length of the cellulose (Klemanleyer *et al*. 1992). Crystalline regions of cellulose, which affect wood tensile strength, were destroyed by *Coriolus versicolor*. The tensile strength of larch flakes decreased during the decaying process.

Fig. 4. Relationship between the infestation time and average mass loss and longitudinal tensile strength with standard deviation

Table 2 shows that the white rot flakes' average tensile strength decreased with continued decay. Average tensile strength decreased greatly within the first 6 weeks. The tensile strength of the flakes also displayed a declining trend, though not as much as in the first 6 weeks. This may be due to decreasing enzyme activity of the white rot fungus after 6 weeks. The longitudinal tensile MOE of the flakes decreased during the decay process, from 18.5 to 11.2 GPa after week 12. The MOE of the samples decreased by 2.5% every two weeks during the brown rot decay period (Cheng 2011). Compared to white rot, brown rot causes a more reduction in wood mechanical properties. This is because brown rot fungi mainly attack cellulose and hemicellulose (Cowling 1961), which determine wood's MOE.

Table 2. Longitudinal Tensile Properties of Larch Flakes after Various Infestation Durations

Infestation Duration (weeks)	Average Longitudinal Tensile Strength (MPa)	Average Longitudinal MOE (GPa)
Non-infested	138.8 (19.7)	18.5 (5.9)
3	122.8 (36.5)	17.5 (3.2)
6	76.9 (16.0)	15.0 (4.2)
9	70.0 (6.9)	12.2 (3.8)
12	60.0 (13.7)	11.2 (3.5)
Mean data (standard deviation)		

Nano-indentation Properties of Infested Larch Flakes

Average nano-indentation hardness of the S2 layer of the cell wall decreased as infestation was prolonged. White rot fungi attack lignin (Cowling 1961), the content of which is directly proportional to the hardness of the wood (Gindl *et al*. 2002). The nano-indentation hardness of the secondary cell wall declined as the lignin content was decreased by *C. versicolor*. It can be seen from Table 3 that the cell wall hardness decreased greatly before 9 weeks had elapsed. This is likely because the enzyme activity of the white rot fungi was high and a certain rate of attack on the lignin component of the wood was maintained during that period. After the ninth week, the enzyme activity of the white rot fungi declined and the rate of lignin depolymerization was slower than in early decay. Therefore, the weight loss rate decreased, and consequently, the nano-indentation hardness loss decreased. As shown in Table 3, the average nano-indentation MOE gradually decreased during the decaying process. Cellulose, which determines the cell wall strength and elongation (Brown 2004), was depolymerized slowly until week 12.

Table 3. Nano-indentation Properties of Larch Cell Wall at Various Infesting Durations

Infestation Duration (weeks)	Average Hardness (MPa)	Average MOE (GPa)
Non-infested	528.47 (57.8)	24.0 (3.14)
3	496.64 (49.2)	21.8 (0.85)
6	469.82 (34.2)	21.3 (1.78)
9	430.42 (28.7)	21.1 (2.11)
12	427.87 (28.0)	17.1 (2.55)
Mean data (standard deviation)		

Relative Crystallinity of Infested Larch Flakes

Figure 5 shows the relative crystallinity of cellulose *vs.* the infestation duration. The relative crystallinity of infested flakes increased during the first three weeks, then slightly decreased, and finally became constant. This is because *C. versicolor* depolymerizes lignin more readily than cellulose, which increases the crystallinity of wood during the first three weeks. The subsequent reduction in lignin content was smaller. The relative crystallinity of cellulose is related to the mechanical properties of wood. The Young's modulus and hardness increase and flexibility decreases with increasing crystallinity (Andersson *et al*. 2003). The cellulose and hemicellulose were degraded, causing the decline in relative crystallinity. The fact that *C. versicolor* attacked the lignin component faster than cellulose at the beginning of decay is consistent with the observations of Pandey and Pitman (2003), who also found that *C. versicolor* destroys the structural components of wood (lignin and carbohydrates) simultaneously, but with a preference for lignin.
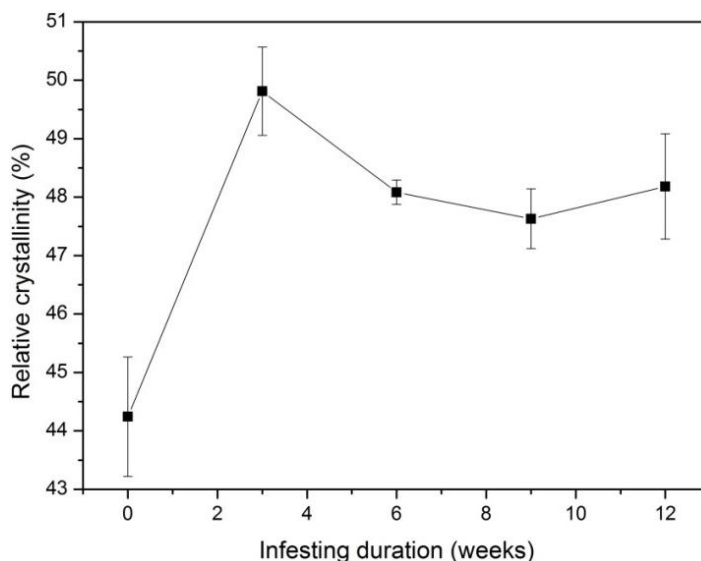

Fig. 5. Relative crystallinity with standard deviation of decaying larch flakes over time

Nitrogen Adsorption Analysis of Infested Larch Flakes

The pore volume is the total volume of all cavities in a material and is related to the components of wood cell wall. The surface area and micropore area increased to 1.33 and 0.53 m^2/g, respectively, and reached a maximum after the third week of fungal decay. The surface area then decreased to 0.71 following the ninth week (Table 4). The pore volume did not change until the ninth week. Pore volume reached a maximum at week 9, indicating that the size of cavities in the cell wall were increased by *C. versicolor*. The increase in surface area was due to the increase in the micropore area *via* cell wall destruction by *C. versicolor*. After the third week, both the surface area and the micropore area decreased.

FTIR Analysis of Infested Larch Flakes

The main chemical components of wood are cellulose, hemicellulose, and lignin. Cellulose is a glucan, in which glucose molecules are connected with β-1-4 glycosidic bonds. Cellulose usually contains thousands of glucose units (Brown 2004). Hemicellulose consists of xylans, xyloglucans, and galactoglucomannans, and is integrated with cellulose in wood cell wall. Lignin is an aromatic polymer found in wood cell wall. It enhances the

hardness of the cell wall and holds the microfibrils together (Gindl *et al.* 2002). Absorption peak locations and assignments for larch are shown in Table 5 (Colom *et al.* 2003; Sarkanen *et al.* 1967).

Table 4. Pore Structure Parameters of Larch Infested with White Rot Fungus for Various Durations

Infestation Duration (weeks)	Surface Area (m^2/g)	Micropore Area (m^2/g)	Pore Volume ($p/p_0 = 0.995$) (cm^3/g)
control sample	0.48	0.23	0.0011
3	1.33	0.53	0.0013
6	0.78	0.34	0.0012
9	0.71	0.31	0.0021

Table 5. Characteristic Bands of the Infrared Spectra of Infested Larch Flakes

Wavenumber (cm^{-1})	Absorption Peak Location and Assignment
1735	C=O stretching in unconjugated ketone, carbonyl, and aliphatic groups (Hemicellulose)
1637	C=O stretching in conjugated carbonyl (Lignin)
1606	Aromatic skeletal stretching and C=O stretching (Lignin)
1509	Aromatic skeletal stretching (Lignin)
1421	Aromatic skeletal combined with C-H in-plane deforming and stretching (Lignin)
1374	Aliphatic C-H in plane deforming and stretching(Cellulose and hemicellulose)
1268	Ar-O stretching in the oxygen bonds of benzene rings (Lignin)
1169	C-O-C stretching (Cellulose and hemicellulose)
1066	C-O stretching (Cellulose, hemicellulose, and lignin)
1028	C-O stretching (Cellulose, hemicellulose, and lignin)
895	Out of phase ring stretching (Cellulose)

In Table 6, the character "I" represents the height of a peak. The ratios are the heights of the lignin peak at 1637 cm^{-1} and the carbohydrate (cellulose and hemicellulose) peak at 1066 cm^{-1} to the heights of the peaks at 1510 cm^{-1} (lignin), 1730 cm^{-1} (hemicellulose), and 895 cm^{-1} (cellulose).

Table 6. Relative Intensities of C=O and C-O Stretching Against Typical Bands

Exposure Period	Relative Peak Intensity Ratios					
	I_{1637}/I_{1510}	I_{1637}/I_{1730}	I_{1637}/I_{895}	I_{1066}/I_{1510}	I_{1066}/I_{1730}	I_{1066}/I_{895}
0 weeks	1.167	2.422	3.769	0.476	0.800	1.538
3 weeks	1.038	2.380	3.375	0.371	0.371	1.208
9 weeks	0.949	2.214	3.321	0.326	0.326	1.142
12 weeks	0.888	1.759	2.968	0.214	0.215	0.718

The FTIR infrared spectra of non-infested and infested samples having undergone various periods of infestation are shown in Fig. 6 and Table 6. Absorption peaks in the infrared spectra varied at different infestation durations. The relative intensities of the peaks at 1637 cm^{-1}, representing the conjugated carbonyl C=O stretching vibrations of lignin, gradually decreased during the decaying process. Values of I_{1637}/I_{1510}, I_{1637}/I_{1730}, and I_{1637}/I_{895} decreased from 1.167 to 1.038, 2.422 to 2.380, and 3.769 to 3.375, respectively,

after week 3. This is because the lignin was attacked intensely and its content was decreased dramatically within the first 3 weeks. The absorption peaks at 1637 cm^{-1} changed little after week 9, likely because the intensity of the attack on lignin decreased. This is consistent with the nano-indentation hardness results, which showed that there was no difference in the hardness between weeks 9 and 12. The peak at 1066 cm^{-1}, representing the C-O functional groups of cellulose and hemicellulose, shows strong stretching absorption for non-infested samples. The intensity decreased during the decaying process. The ratios I_{1066}/I_{1510}, I_{1066}/I_{1730}, and I_{1066}/I_{895} decreased from 0.476 to 0.214, 0.800 to 0.215, and 1.538 to 0.718, respectively, from the control samples to the samples infested for 12 weeks, indicating that cellulose and hemicellulose experienced severe damage from the white rot fungus. The FTIR results confirmed that *C. versicolor* attacked both lignin and cellulose at the same time.

Relative intensities of the peaks at 1606 cm^{-1} and 1421 cm^{-1} became stronger during the fungal infestation because lignin was degraded into smaller molecules. With the development of fungal infestation, the peak at 1028 cm^{-1} (representing C-O stretching of cellulose, hemicellulose, and lignin) increased and the peak at 1066 cm^{-1} (representing the C-O stretching of cellulose and hemicellulose) decreased. This may be due to the rupture of C=O bonds in lignin at 1637 cm^{-1}, to create C-O bonds. The structural damage of the lignin resulted in a decrease in the nano-indentation hardness.
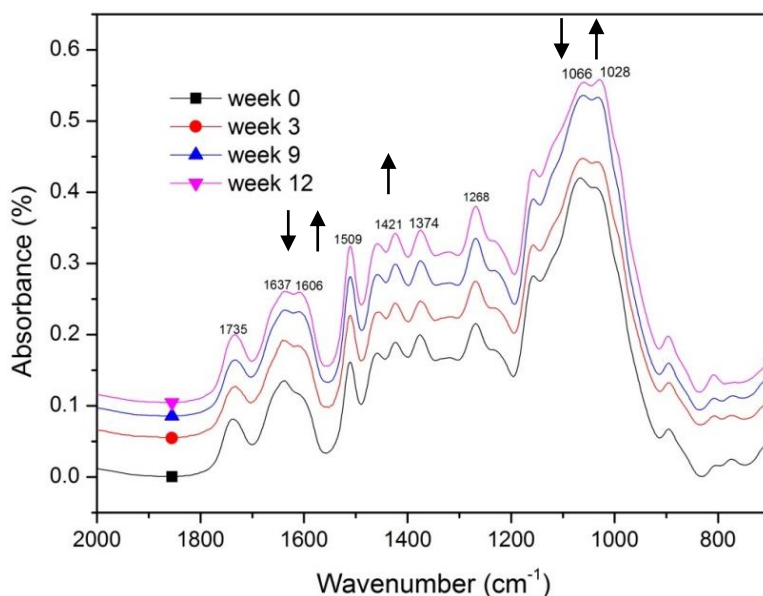
Fig. 6. FTIR spectra of larch decay over various time periods

CONCLUSIONS

1. The mass loss of infested larch flakes was greater during the early stages of decay, most notably during the first three weeks. The rate of mass loss slowed after the flakes had lost more than 10% of their initial mass.

2. The mechanical strength of the infested flakes decreased. The tensile strength and tensile MOE of wood flakes decreased from 138.8 to 60.0 MPa and 18.5 to 11.2 GPa, respectively, after 12 weeks of fungal infestation. At the same time, the nano-

indentation hardness and MOE deceased from 528.47 to 427.87 MPa and 24.0 to 17.1 GPa, respectively.

3. The relative crystallinity increased from 44.24 to 49.81% during the first three weeks of fungal infestation. The surface area and micropore area of the wood's cells reached maxima of 0.85 and 0.30 m^2/g, respectively, after week 3.

4. The results of this study indicate that *C. versicolor* intensely attacked lignin during the first three weeks of decay. Absorbance intensities at 1637 cm^{-1} (representing lignin) and 1066 cm^{-1} (representing cellulose and hemicellulose) weakened with increasing duration of infestation.

ACKNOWLEDGMENTS

REFERENCES CITED

ASTM D 2017 (2005). "Standard method of accelerated laboratory test of natural decay resistance of wood," *American Society for Testing and Materials*, West Conshohocken, PA.

Andersson, S., Serimaa, R., Paakkari, T., Pekka, S., and Pesonen, E. (2003). "Crystallinity of wood and size of cellulose crystallites in Norway spruce (*Picea abies*)," *The Japan Wood Research Society* 49(6), 531-537.

Berben, S. A., Rademacher, J. P., Sell, L., and Easty, D. B. (1987). "Estimation of lignin in wood pulp by diffuse reflectance Fourier transform infrared spectrometry," *TAPPI Journal* 70(1), 129-133.

Blanchette, R. A., Otjen, L., Effland, M. J., and Eslyn, W. E. (1985). "Changes in structural and chemical components of wood delignified by fungi," *Wood Science and Technology* 19(1), 35-46.

Brown, R. M. (2004). "Cellulose structure and biosynthesis: What is in store for the 21st Century," *Journal of Polymer Science* 42(3), 487-495.

Brunauer, S., Emmett, P. H., and Teller, E. (1938). "Adsorption of gases in multimolecular layers," *Journal of the American Chemical Society* 60(2), 309-319.

Buchert, J., Ratto, M., Mustranta, A., Suurnakki, A., Ekman, R., Spetz, P., Siika-aho, M., and Viikari, L. (1998). "Enzymes for the improvement of paper machine runnability," in: *Proceedings of the Seventh International Conference of Biotechnology in the Pulp and Paper Industry*, CPPA, Montreal, Canada, pp. A225-A228.

Curling, S. F., Clausen, C. A., and Winandy, J. E. (2002). "Relationships between mechanical properties, weight loss, and chemical compositions of wood during incipient brown rot decay," *Forest Products Journal* 52(7-8), 34-39.

Chang, S., Hu, J., Clair, B., and Quignard, F. (2011). "Pore structure characterization of poplar tension wood by nitrogen adsorption-desorption method," *Scientia Silvae Sinicae* 47(10), 134-140.

Cheng, X. B. (2011). *The Influence of Incipient Brown Rot on the Properties of Chinese Fir at Macroscopic and Tissue Level*, M.S. thesis, Chinese Academy of Forestry, Beijing.

Colom, X., Carrillo, F., Nogués, F., and Garriga, P. (2003). "Structural analysis of photodegraded wood by means of FTIR spectroscopy," *Polymer Degradation and Stability* 80(3), 543-549.

Cowling, E. B. (1961). *Comparative Biochemistry of the Decay of Sweetgum Sapwood by White-rot and Brown-rot Fungi*, Government Printing Office, Washington, DC.

Cutter, B. E., McGinnes, E. A. J., and Schmidt P. W. (1980). "X-ray scattering and X-ray diffraction techniques in studies of gamma-irradiated wood," *Wood and Fiber Science* 11(4), 228-232.

Davis, M. F., Schroeder, H. A., and Maciel, G. E. (1994). "Solid state ^{13}C nuclear magnetic resonance studies of wood decay. Ⅱ White rot decay of paper bitch," *Holzforschung* 48(3), 186-192.

Erwin, E. J. K., Jim, A. F., and Thomas, W. J. (1995). "Increasing ligninolytic enzyme activities in several white-rot basidiomycetes by nitrogen-sufficient media," *Bioresource Technology* 53(2), 133-139.

Fackler, K., Gradinger, C., Hinterstoisser, B., Messner, K., and Schwanninger, M. (2006). "Lignin degradation by white rot fungi on spruce wood shavings during short-time solid-state fermentations monitored by near infrared spectroscopy," *Enzyme and Microbial Technology* 39(7), 1476-1483.

Fackler, K., Stevanic, J. S., Ters, T., Hinterstoisser, B., Schwanninger, M., and Salmén, L. (2010). "Localisation and characterisation of incipient brown-rot decay within spruce wood cell walls using FT-IR imaging microscopy," *Enzyme and Microbial Technology* 47(6), 257-267.

Fackler, K., Stevanic, J. S., Ters, T., Hinterstoisser, B., Schwanninger, and M., Salmén, L. (2011). "FT-IR imaging microscopy to localise and characterize simultaneous and selective white-rot decay within spruce wood cells," *Holzforschung* 65(3), 411-420.

Fagerlund, G. (1973). "Determination of specific surface by the BET method," *Matériaux et Construction* 6(3), 239-245.

Gibson, L. J., and Ashby, M. F. (1997). *Cellular Solids, Structure and Properties*, Cambridge University Press, New York.

Gindl, W., Gupta, H. S., and Grünwald, C. (2002). "Lignification of spruce tracheid secondary cell walls related to longitudinal hardness and modulus of elasticity using nano-indentation," *Canadian Journal of Botany* 80(10),1029-1033.

Hermans, P. H., and Weidinger, A. (1948). "Quantitative X-ray investigations on the crystallinity of cellulose fibers," *Journal of Applied Physics* 19(5), 491-506.

Jones, T., Meder, R., Low, C., Ocallahan, D., Chittenden, C., Ebdon, N., Thumm, A., and Riddell, M. (2011). "Natural durability of the heartwood of coast redwood [*Sequoia sempervirens* (D. Don) Endl.] and its prediction using near infrared spectroscopy," *Journal of Near Infrared Spectroscopy* 19(5), 381-389.

Kaufmann, J. (2010). "Pore space analysis of cement-based materials by combined Nitrogen sorption - Wood's metal impregnation and multi-cycle mercury intrusion," *Cement & Concrete Composites* 32(7), 514-522.

Klemanleyer, K., Agosin, E., Conner, A. H., and Kirk, T. K. (1992). "Changes in molecular-size distribution of cellulose during attack by white rot and brown rot fungi," *Applied and Environmental Microbiology* 58(4), 1266-1270.

Kojiro, K., Miki, T., Sugimoto, H., Nakajima, M., and Kanayama, K. (2010). "Micropores and mesopores in the cell wall of dry wood," *Journal of Wood Science* 56(2), 107-111.

Li, G. Y., Huang, L. H., Hse, C. Y., and Qin, T. F. (2011). "Chemical compositions, infrared spectroscopy, and X-ray diffractometry study on brown-rotted woods," *Carbohydrate Polymers* 85(3), 560-564.

Perez, V., Troya, M. T., Martinez, A. T., Gonzalez-Vila, F. J., Arias, E., and Gonzalez, A. E. (1993). "In vitro decay of *Aextoxicon punctatum* and *Fagus sylvatica* woods by white and brown rot fungi," *Wood Science and Technology* 27(4), 295-307.

Pandey, K. K., and Pitman, A. J. (2003). "FTIR studies of the changes in wood chemistry following decay by brown-rot and white-rot fungi," *International Biodeterioration & Biodegradation* 52(3), 151-160.

Rodrigues, J., Faix, O., and Pereira, H. (1998). "Determination of lignin content of *Eucalyptus globulus* wood using FTIR spectroscopy," *Holzforschung* 52(1), 46-50.

Sarkanen, K. V., Chang, H. M., and Ericsson, B. (1967). "Species variation in lignins I. Infrared spectra of guaiacyl and syringyl models," *TAPPI Journal* 50(11), 572-575.

Schultz, T. P., Templeton, M. C., and McGinnis, G. D. (1985). "Rapid determination of lignocellulose by diffuse reflectance Fourier transform infrared spectrometry," *Analytical Chemistry* 57(14), 2867-2869.

Schwanninger, M., Hinterstoisser, B., Gierlinger, N., Wimmer, R., and Hanger, J. (2004). "Application of Fourier transform near infrared spectroscopy (FT-NIR) to thermally modified wood," *European Journal of Wood and Products* 62(6), 483-485.

Shao, Z., and Li, K. (2006). "The effect of fiber surface lignin on interfiber bonding," *Journal of Wood Chemistry and Technology* 26(3), 231-244.

Solár, R., Kurjatko, S., Mamoň, M., Košíková, B., Neuschlová, E., Výbohová, E., and Hudec, J. (2007). "Selected properties of beech wood degraded by brown-rot fungus *Coniophora puteana*," *Drvna Industrija* 58(1), 3-11.

Westermarck, S., Juppo, A. M., Kervinen, L., and Ylruusi, J. (1998). "Pore structure and surface area of mannitol powder, granules and tablets determined with mercury porosimetry and nitrogen adsorption," *European Journal of Pharmaceutics and Biopharmaceutics* 46(1), 61-68.

Wilcox, W. W. (1978). "Review of literature on the effects of early stages of decay on wood strength," *Wood and Fiber* 9(4), 252-257.

Wimmer, R., Lucas, B. N., Tsui, T. Y., and Oliver, W. C. (1997). "Longitudinal hardness and Young's modulus of spruce tracheid secondary walls using nanoindentation technique," *Wood Science and Technology* 31(2), 131-141.

Winandy, J. E, and Morrell, J. J. (1993). "Relationship between incipient decay, strength, and chemical composition of Douglas-fir heartwood," *Wood and Fiber Science* 25(3), 278-288.

Yu, Y., Fei, B. H., Wang, H. K., and Tian, G. L. (2010). "Longitudinal mechanical properties of cell wall of Masson pine (*Pinus massoniana* Lamb) as related to moisture content: A nanoindentation study," *Holzforschung* 65(1), 121-126.